ACS EARTH AND SPACE CHEMISTRY

Article

Cite This: ACS Earth Space Chem. 2018, 2, 31−37

Absorbing Refractive Index and Direct Radiative Forcing of Atmospheric Brown Carbon over Gangetic Plain

P. M. Shamjad,[†] R. V. Satish,[‡] Navaneeth M. Thamban,[†] N. Rastogi,[‡] and S. N. Tripathi*[,†,§]

[†]Department of Civil Engineering and [§]Centre for Environmental Science and Engineering, Indian Institute of Technology Kanpur, Kanpur, Uttar Pradesh 208016, India

[‡]Geosciences Division, Physical Research Laboratory, Ahmedabad, Gujarat 380009, India

Supporting Information

ABSTRACT: Atmospheric carbonaceous aerosols consisting of black carbon and organic carbon influence Earth's radiative balance by interacting with solar radiation. A subset of organic aerosols known as brown carbon is absorbing in nature and poorly characterized in terms of optical properties. Brown carbon can warm the local and regional atmosphere depending upon its absorbing capacity, mixing state, and meteorological conditions. We report a diurnal spectral absorbing refractive index of brown carbon over North India and its influence on regional radiative forcing. Measurements show the presence of highly absorbing brown carbon consisting of soluble and non-soluble fractions having distinct spectral absorption. The brown carbon refractive index at 365 nm shows a 50% reduction during daytime when compared to nighttime as a result of combined effects of reduced primary emissions and photobleaching/volatilization. Brown carbon and the lensing effect as a result of a thin absorbing coating exert a forcing of −0.93 ± 0.27 and 0.13 ± 0.06 W m^{-2}, respectively, at the top of atmosphere. Externally mixed absorbing organic carbon in radiative forcing calculations produces 48% less cooling when compared to the forcing induced by scattering organic carbon. The presence of internally mixed absorbing organic carbon as a shell over black carbon induces 31% more warming compared to a similar shell made of scattering organic carbon. Overall results suggest that brown carbon and the lensing effect need to be included in global climate models while calculating radiative forcing parameters.

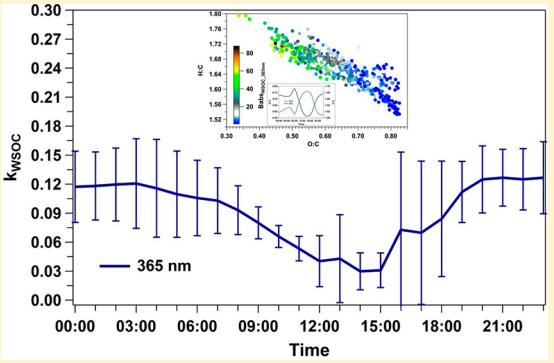

KEYWORDS: *carbonaceous aerosols, mixing state, absorbing refractive index, radiative forcing, biomass burning*

INTRODUCTION

Carbonaceous aerosols having diverse optical and physical properties are of particular interest in climate studies as a result of their capacity to warm the atmosphere.[1] Unlike black carbon (BC), absorption due to brown carbon (BrC) is not well-characterized as a result of the large heterogeneity in its optical properties arising from its diverse sources and involvement in secondary processes, such as photochemical aging.[2] Primary emissions, for example, fossil fuel combustion and biomass burning, contribute mainly to the atmospheric abundance of carbonaceous aerosols. Global emission inventory studies report annual emissions of 8 and 33.9 Terra gram (Tg) for BC and organic carbon (OC), respectively, in which open biomass burning contributes up to 42% for BC and 74% for OC.[3] In regions such as Central Africa, China, and Northern India, open biomass burning is a dominant source for OC.[4] The perturbation to the Earth atmosphere radiative balance as a result of aerosols is generally expressed in terms of radiative forcing (W m^{-2}), which is a measure of the change in net radiative flux at the top of atmosphere (TOA).[5] The radiative forcing due to BrC aerosols is subject to large uncertainty as a result of a lack of accurate knowledge of (a) the optical and physical properties of BrC and (b) the mixing state of BC and BrC.[6] Because BC and OC are usually co-emitted, their mixing state can significantly influence the overall absorption, thus further influencing forcing estimates. The term "mixing state" is used to indicate the physical state of aerosols in the atmosphere and is divided into external and internal mixing. In external mixing, aerosols co-exist as individual particles. On the other hand, in internal mixing, aerosols are homogeneously mixed with each other in various configurations (core−shell, spheroids, etc.).[7] In core−shell internal mixing, an insoluble aerosol species (BC) becomes coated with a soluble species (organics and/or inorganics). Core−shell-type mixing leads to enhancement in absorption as a result of the shell acting as a lens (lensing effect).[8,9]

Absorption due to BrC can reduce the net cooling effect caused by scattering aerosols or even induce warming in areas with large-scale biomass burning.[4] A number of global modeling studies[6,10,11] considering absorbing OC aerosols report 0.11 W m^{-2} warming at TOA when compared to purely

Received: June 29, 2017
Revised: November 16, 2017
Accepted: November 29, 2017
Published: November 29, 2017

DOI: 10.1021/acsearthspacechem.7b00074
ACS Earth Space Chem. 2018, 2, 31−37

scattering OC. Two other studies[12,13] report higher warming values (0.24−0.4 W m^{-2}) for direct radiative forcing by absorbing OC. Another study, conducted over the Central U.S.A. using aircraft sampling, reports a 20% reduction in TOA cooling when absorbing OC is considered.[14] Water-soluble organic carbon (WSOC) measured from New Delhi[15] and Gangetic plain outflow[16,17] were reported to contribute 6 and 35%, respectively, to solar absorption relative to that of BC. The lensing effect also induces a radiative effect in the atmosphere depending upon the type of material coated and its thickness. A study[18] shows that externally mixed absorbing OC and the lensing effect increase the global mean direct forcing from −0.46 to +0.05 W m^{-2}. However, global climate model-based OC forcing estimates have large uncertainties as a result of the uncertainty associated with OC refractive index and its assumed mixing state.[2,4] A number of studies reported (measured or modeled or both) absorbing refractive index for atmospheric and laboratory-generated OC.[19−23] These studies used various methods, such as closure between measured and modeled absorption,[20,23,24] liquid extraction,[21] and electron microscopy,[22] to quantify the refractive index of OC. The large variation (from 0.0009[21] to 0.27[22] at ∼550 nm) in the reported refractive index values shows the heterogeneous nature of OC in the atmosphere. Accurate measurement of the BrC refractive index on a regional scale is necessary to calculate its contribution to total aerosol absorption.

The overall goal of this study is to quantify the absorbing refractive indices of WSOC and total OC and identify their spectral dependence. Using this refractive index and simultaneously measured physical properties as input, species-specific radiative forcing is calculated to understand the effects of absorbing OC and the lensing effect on the radiative balance. The influence of varying shell thickness on net radiative forcing is also calculated.

EXPERIMENTAL SECTION

Sampling Details. Data presented in this study were collected during a high aerosol loading winter season (from December 28, 2015 to January 31, 2016) in Kanpur, an urban India city located in the Gangetic plain (GP). The GP is known for its high aerosol loading as a result of open biomass burning, especially during the winter season.[25] The mean ± standard deviation of the sub-micrometer aerosol mass concentration during the campaign was found to be 184 ± 108 $\mu g\ m^{-3}$, which indicates high loading conditions in terms of air quality standards.[26]

Instrumentation. Figure S1 of the Supporting Information shows a schematic of the instrument setup used to collect aerosols in this study. An Aerodyne high-resolution time-of-flight aerosol mass spectrometer (HR-ToF-AMS) and TSI scanning mobility particle sizer (SMPS) were operated in atmospheric and thermally denuded (∼300 °C) conditions with a 10 min switching interval to collect sub-micrometer chemical composition and particle size distributions. Aerosols were pre-dried to a relative humidity (RH) of <10% using a silica gel dryer to apply uniform collection efficiency in HR-ToF-AMS. A single particle soot photometer (SP2) was used to measure BC mass and size distributions. A particle-into-liquid sampler (PILS) with an air inlet cutoff diameter of 2.5 μm ($PM_{2.5}$) was used to extract atmospheric aerosols in ultrapure water, which was then passed through a liquid waveguide capillary cell (LWCC) and total organic carbon (TOC) analyzer for measuring spectral absorbance and mass concentration of WSOC, respectively, with a 4 min frequency. The absorbing refractive index of WSOC (k_{WSOC}) was calculated online using this absorbance and WSOC mass concentration (see the Methods). Two high-volume samplers (HVSs) with cutoff diameters of 2.5 and 1.0 μm ($PM_{2.5}$ and PM_1) were also operated to collect particles on pre-combusted Tissuquartz filters, which were then extracted with methanol to measure spectral absorbance of OC. This absorbance was used to calculate the absorbing refractive index of OC (k_{OC}) for both $PM_{2.5}$ and PM_1 offline. Values of k_{WSOC} and k_{OC} were calculated over a range of wavelengths (300−700 nm) (for more details on instrument description and calibration, see the Supporting Information).

METHODS

HR-ToF-AMS and SP2 Data Analysis. The HR-ToF-AMS measured unit mass resolution (UMR) spectra were analyzed using standard SQUIRREL software package (version 1.56D) initially. High-resolution (HR) analysis was performed using PIKA (version 1.15D) with the help of peak fitting algorithms up to a m/z value of 150. A uniform collection efficiency of 0.45 was used for calculating the final mass concentrations.[27] Because data collection frequency varied with instruments, all online measured data were hourly averaged for analysis. The SP2 data analysis was performed using a SP2 data analysis toolkit (version 4.1000a) by combining broadband high- and low-gain channels.

Calculation of WSOC Refractive Index Online. An automated PILS−LWCC−TOC system with a $PM_{2.5}$ inlet was used to simultaneously measure spectral absorbance (A_λ) and mass concentration of WSOC with a 4 min time resolution. In PILS, ambient particles were extracted with high-purity water, filtered using a 0.45 μm filter, and then sent to LWCC (0.5 mL min^{-1}) and TOC (0.4 mL min^{-1}) using a peristaltic pump. Details of these measurements are published elsewhere.[28,29] The sampling line was diverted every day through a high-efficiency particulate air (HEPA) filter for 30 min to correct for background values. Absorbance was recorded for a wide range of wavelengths (250−700 nm). To account for baseline drifting during long sampling duration, all A_λ values were referenced to A_{700}. Absorbance and mass concentrations were hourly averaged for further analysis. Previous studies reported various correction factors, such as 0.69,[30] 0.75,[31] and 2,[21] for converting the bulk solution absorption to atmospheric absorption by comparing the measured and Mie-theory-derived absorption. A similar calculation showed a correction factor of 1.9 in this study, and the same was used to obtain BrC atmospheric absorption. The spectral absorption coefficient for the solutions (water and methanol) ($B_{abs\text{-}\lambda}$) in Mm^{-1} was calculated as follows:

$$B_{abs\text{-}\lambda} = (A_\lambda - A_{700})\frac{V_l}{V_a l}\ln(10) \quad (1)$$

where V_l is the flow rate of liquid through PILS (0.7 mL min^{-1}), V_a is the flow rate of air through PILS (16.7 L min^{-1}), and l is the absorbing path length (2 m). From $B_{abs\text{-}\lambda}$, the WSOC refractive index (k_{WSOC}) was calculated as

$$k_{WSOC} = \frac{\rho\lambda(B_{abs\text{-}\lambda})}{4\pi(WSOC)} \quad (2)$$

where ρ is the density of WSOC (1.5 g cm^{-3}).

DOI: 10.1021/acsearthspacechem.7b00074
ACS Earth Space Chem. 2018, 2, 31−37

Calculation of OC Refractive Index Offline. Two HVSs of $PM_{2.5}$ and PM_1 size cutoff were operated during the campaign to collect aerosols on preheated quartz filters. The $PM_{2.5}$ sampler was operated with a flow rate (V_a) of 1100 L min^{-1} and a sampling frequency of 23 h to collect aerosols on a filter of area of 400 cm^2. The PM_1 sampler collected aerosols on a filter with a diameter of 47 mm and operated with a flow rate (V_a) of 215 L min^{-1} with varying sampling frequency between 4 and 6 h. A total of 59 $PM_{2.5}$ and 79 PM_1 filters were collected during the entire campaign. Filters collected from both samplers were kept in a freezer until analysis. One punch (area of 0.7 cm^2 for $PM_{2.5}$ and 1.5 cm^2 for PM_1) from both filters was dissolved in a known volume (V_l) of methanol to extract OC. Another punch of 1.5 cm^2 area was analyzed in a Sunset OC-EC analyzer[32] through the NIOSH method for OC mass concentration. Methanol-extracted OC samples were injected into LWCC for spectral absorbance. The absorption coefficient and refractive indices were then calculated using eqs 1 and 2. Because only a punch from the whole filter was used for analysis, the calculated absorption coefficients were multiplied by the ratio of filter area/punch area.

Coating Factor (CF) Determination. The CF is defined as the ratio of the diameter of the core−shell particle ($D_{core+shell}$) to the diameter of the core particle (D_{core}).[20]

$$CF = \frac{D_{core+shell}}{D_{core}} \tag{3}$$

A scanning mobility particle sizer (TSI, EC-3080, and CPC-3776) was operated to measure the particle size distribution under atmospheric and denuded conditions with 10 min switching frequency. The mode of the atmospheric particle size distribution was used as the diameter of the core−shell particle ($D_{core+shell}$), and the mode of the denuded size distribution was used as the diameter of the core particle (D_{core}). Figure S2 of the Supporting Information shows a representative size distribution of atmospheric and denuded aerosols with mode diameters. This method of CF determination assumes the entire aerosol population to be internally mixed and that the denuding process removes all volatile species. Because the majority of aerosols over the sampling site are internally mixed (up to 75%),[33] this method can be used to determine the CF.

Mie Modeling. It was assumed that particles are spherical in shape and that the Mie theory could be used to calculate the optical properties of OC and BC + shell. The Mie calculation routines used in this study were developed by Bond et al.[8] with inputs from Matzler et al.,[34] which require size distribution and refractive index for the calculation of optical properties. The OC size distribution was derived using the time-of-flight data from HR-ToF-AMS, and the same for BC was measured directly using SP2. Measured spectral refractive indices were used for OC, and previously reported values were used for BC.[19] A perfect core−shell structure was assumed, where BC acts as a core and a homogeneous mixture of OC and inorganics makes the shell. The net refractive index of the shell was calculated using the volume mixing rule, where measured k_{OC} values were used and inorganics were considered to be completely scattering. The steps followed in the net shell refractive index are described in the Supporting Information.

Calculation of Relative Forcing Efficiency (RFE). RFE is defined as the shortwave radiative forcing per unit optical depth at TOA as a result of a uniform, optically thin layer of aerosols in the lower troposphere. RFE is calculated as per the following equation[35] for dry aerosols:

$$\mathrm{RFE} = \frac{\Delta F}{\mathrm{AOD}} = SD(1 - A_{cld}){T_{atm}}^2(1 - R_{sfc})^2 \left[2R_{sfc}\frac{1 - \mathrm{SSA}}{(1 - R_{sfc})^2} - \beta(\mathrm{SSA})\right] \tag{4}$$

where ΔF is the change in net solar flux at the TOA as a result of aerosols, AOD is the aerosol optical depth, S is the solar constant (1370 W m^{-2}), D is the fractional day length (0.5), A_{cld} is the fractional cloud cover (0.6), T_{atm} is the solar atmospheric transmittance (0.76), R_{sfc} is surface albedo (0.15), SSA is single scattering albedo, and β is the fraction of scattered sunlight that is scattered into the upward hemisphere, calculated as eqs 5 and 6. The term "g" indicates the asymmetric parameter, and the term "b" denotes the ratio of back scattering coefficient/total scattering coefficient.

$$b = \frac{1 - g^2}{2g}\left[\frac{1}{\sqrt{1 + g^2}} - \frac{1}{1 + g}\right] \tag{5}$$

$$\beta = 0.082 + 1.85b - 2.97b^2 \tag{6}$$

The SSA and g values for OC and BC + shell were derived from the Mie model using measured size distribution and refractive index.

Calculation of Species-Specific Aerosol Optical Depth (AOD) Determination. Individual contributions from OC, BC, and BC + shell to total AOD were calculated using a previously reported procedure.[4,36] Because the mass fraction of fine mode dust was negligible in Kanpur during the winter season,[37] absorption from the same was not considered. Total absorbing aerosol optical depth ($AAOD_{\lambda o\_total}$) was calculated from AERONET measured total AOD ($AOD_{\lambda o\_total}$) and single scattering albedo ($SSA_{\lambda o}$) at a reference wavelength (λ_0) of 405 nm using eq 7.

$$\mathrm{AAOD}_{\lambda o\_total} = \mathrm{AOD}_{\lambda o\_total}(1 - \mathrm{SSA}_{\lambda o}) \tag{7}$$

AAOD values for OC ($AAOD_{\lambda o\_OC}$) and BC ($AAOD_{\lambda o\_BC}$) were calculated from $AAOD_{\lambda o\_total}$ by solving eq 8 for 405 and 781 nm with values of absorption angstrom exponents (AAEs) of 1.21 ± 0.2 (for total[36] with 405−781 nm wavelength pair), 1 (for BC[19]), and 7.8 ± 0.6 (for OC using measured spectral absorption with 405−781 nm wavelength pair).

$$\mathrm{AAOD}_{\lambda o\_total}\left(\frac{\lambda}{\lambda o}\right)^{-\mathrm{AAE}_{total}} = \mathrm{AAOD}_{\lambda o\_OC}\left(\frac{\lambda}{\lambda o}\right)^{-\mathrm{AAE}_{OC}} + \mathrm{AAOD}_{\lambda o\_BC}\left(\frac{\lambda}{\lambda o}\right)^{-\mathrm{AAE}_{BC}} \tag{8}$$

AAOD for OC and BC at different wavelengths were calculated using eq 9.

$$\mathrm{AAOD}_{\lambda\_BC/BrC} = \mathrm{AAOD}_{\lambda o\_BC/BrC}\left(\frac{\lambda}{\lambda o}\right)^{-\mathrm{AAE}_{BC/BrC}} \tag{9}$$

OC- and BC-specific AOD values were back-calculated from $AAOD_{\lambda\_OC}$ and $AAOD_{\lambda\_BC}$ using eq 7 by substituting SSA for OC, BC, and BC + shell (derived using the Mie theory).

DOI: 10.1021/acsearthspacechem.7b00074
ACS Earth Space Chem. 2018, 2, 31−37

RESULTS AND DISCUSSION

Absorbing Refractive Index. The campaign mean ± standard deviation of WSOC/OC ratio is found to be 0.32 ± 0.15, indicating the dominance of the water-insoluble OC fraction. Figure 1 shows the mean values of k_{WSOC} and k_{OC} for

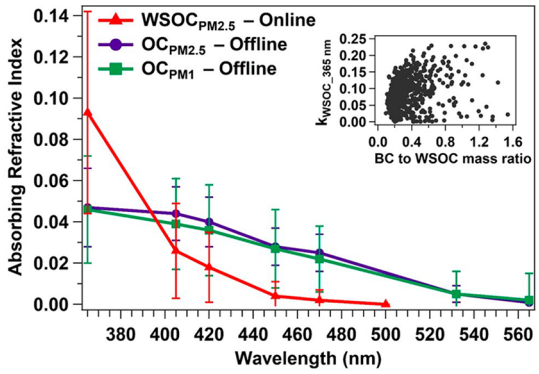

Figure 1. Campaign-averaged spectral absorbing refractive index of $WSOC_{PM_{2.5}}$, $OC_{PM_{2.5}}$, and OC_{PM_1}. Error bars indicate one standard deviation.

selected wavelengths (see Table S1 of the Supporting Information for values). The k_{OC} values reported here are 6−8 times higher than previously reported values from elsewhere.[20,21] The similar k_{OC} values derived from $PM_{2.5}$ and PM_1 filters indicate the similarity in $PM_{2.5}$ and PM_1 in terms of OC composition. k_{WSOC} at 365 nm from this study is up to 20 times higher than another atmospheric study.[21] However, these values are smaller when compared to refractive indices of lab-generated pure biomass or wood smoke.[19,38] Distinct spectral dependence in k_{WSOC} and k_{OC} is also observed from Figure 1. At 365 nm, k_{WSOC} is 1.8 times higher than that of OC but sharply decreases to values smaller than k_{OC} at 405 nm and to negligible absorption beyond 470 nm. However, OC shows non-negligible absorption up to 565 nm. Figure 1 shows that absorption from WSOC is limited to a narrow spectral range (365−470 nm); however, OC has a wider range of absorption (365−565 nm), indicating that the net absorption from OC depends upon the relative abundance and absorptive characteristics of WSOC. Beyond 565 nm, absorption from organic species ceases to exist. Saleh et al.[23] reported a positive relation between BC/organic mass ratio and absorption refractive index, which can be used to predict the absorption capacity of lab-generated organics. No such relationship is found in this study (inset of Figure 1), limiting the wider suitability of BC/organic mass ratio in absorption estimation for aged atmospheric OC.

A strong diurnal variation is observed in k_{WSOC} throughout the campaign (Figure 2), which is more pronounced at 365 nm with a high nighttime mean value of 0.12 ± 0.03 and low daytime mean value of 0.03 ± 0.02. For higher wavelengths (420 nm), daytime k_{WSOC} values are close to zero. This diurnal pattern can be explained in terms of WSOC evolution in the atmosphere. Mass concentrations of WSOC and OC show a diurnal trend similar to that of k_{WSOC}. As a result of primary emissions from biofuel burning and vehicular traffic, increased mass concentrations are observed between 6:00 a.m. and 9:00 a.m., which drop to half of their nighttime values after 11:00 a.m. This reduction in mass concentration from midday to afternoon is due to the combined effect of boundary layer expansion and reduced primary emissions. A positive matrix

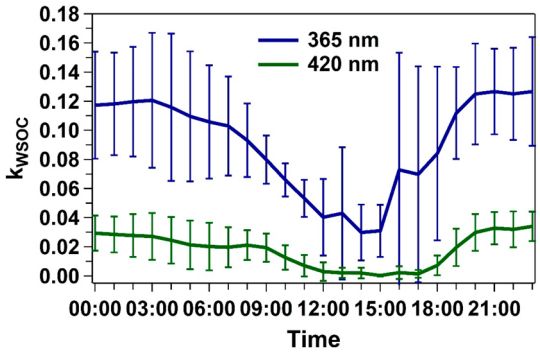

Figure 2. Campaign-averaged diurnal variation of k_{WSOC} at 365 and 420 nm. Error bars represent one standard deviation.

factorization (PMF)[39] analysis is performed on the organic spectra to identify the various factors contributing to bulk organic aerosol loading. The analysis shows both primary and secondary organic aerosol (SOA) factors with diurnal trends similar to that of WSOC, OC mass concentration, and k_{WSOC} (Figure S3 of the Supporting Information). The SOAs produced during daytime are oxygenated organic aerosols (OOAs) with a high oxygen/carbon (O/C) ratio and a low hydrogen/carbon (H/C) ratio.[40] Even though the OOA fraction dominates the bulk organic loading (up to 78%; inset of Figure S3 of the Supporting Information), a previous study from the same locations shows that it contributes less to the total organic absorption.[41] A van Krevelen diagram[42] with color-coded WSOC absorption values indicates that highly absorbing organics are associated with low O/C and high H/C (primary organics) compounds (Figure S4 of the Supporting Information). Therefore, the low k_{WSOC} values during daytime are attributed to least absorbing or completely scattering OOAs and primary organics. Another possible mechanism behind the low k_{WSOC} values during daytime is photobleaching, which effectively reduces the absorbing capacity of organic aerosols.[29,43,44]

Radiative Forcing. To understand the effect of BrC on radiative forcing, a modified forcing parameter, RFE (W m^{-2}) is estimated. Previous studies[35,45] estimated RFE for lab-generated aerosols with measured absorption properties. This study reports RFE for atmospheric BrC, providing a more realistic value of BrC forcing. Two cases of RFE calculations are made for only OC and BC + shell aerosol by considering two optical situations (i) a purely scattering case (k = 0) and (ii) an absorbing case (k = measured refractive index from this study). The difference between the scattering and absorbing RFE values underlines the importance of considering BrC in RFE calculations. panels a and b of Figure 3 show the RFE values for only OC and BC + shell, respectively, for cases i and ii along with the difference between two cases (ΔRFE), $RFE_{absorbing} - RFE_{scattering}$ (Table S2 of the Supporting Information for values). Positive values of ΔRFE as a result of BrC absorption for only OC and BC + shell are more pronounced at lower wavelengths, indicating an offsetting to the cooling effect caused by scattering OC. The ΔRFE for OC values at 405 nm in this study is 14.77 W m^{-2} compared to 3.1 W m^{-2} from a lab study[45] with pure biomass burning smoke (k = 0.015), indicating the highly absorbing nature of organics in GP. Because the shell here is assumed to be a mixture of organic and inorganics, BrC present in the shell can influence RFE. Figure 3b shows the RFE values for BC + shell for a campaign-

DOI: 10.1021/acsearthspacechem.7b00074
ACS Earth Space Chem. 2018, 2, 31−37

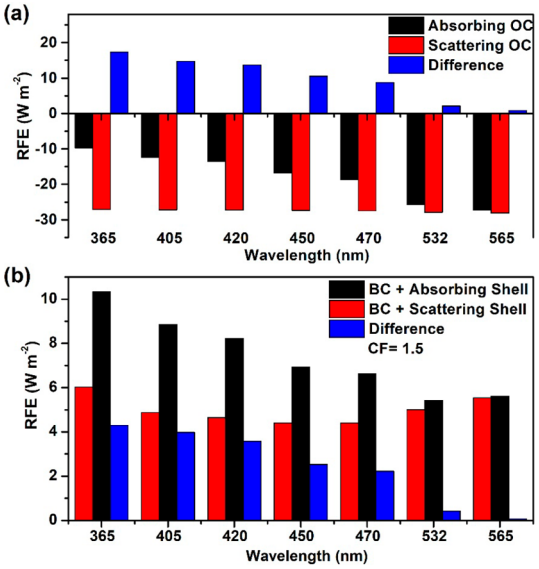

Figure 3. RFE values considering absorbing and scattering and their difference, $RFE_{absorbing} - RFE_{scattering}$ (ΔRFE), for (a) OC and (b) shell over BC. In panel b, the difference indicates the effect of the coating as a result of absorbing aerosols on RFE values.

averaged CF (see the Methods) of 1.50, which is close to the previously reported value of 1.6 using optical closure[41] from the same sampling site.

In case ii, RFE values when integrated over the BrC absorbing wavelength range (365−565 nm) are −3.7 ± 0.83, 3.08 ± 0.37, and 1.43 ± 0.21 W m^{-2} for OC, BC, and BC + average shell, respectively. The similar RFE integrated values under the scattering case (case i) show a value of −5.5 ± 0.33 and 0.98 ± 0.06 W m^{-2} for OC and BC + average shell, respectively. Therefore, externally mixed absorbing OC induces 48% less cooling, and absorbing OC inside the shell of a core−shell structure increases the warming by 31%. Further radiative forcing values of OC, BC, and BC + shell are calculated by multiplying the case ii RFE values with their individual AOD. The individual species-wise AOD is calculated from total AOD values taken from the Kanpur AERONET station using the modified approach[36] of Chung et al.[4] (see the Methods). Wavelength-integrated AOD for OC, BC, and BC + average shell is 0.251 ± 0.05, 0.062 ± 0.03, and 0.078 ± 0.025, respectively. The calculated radiative forcing values from OC and BC are −0.93 ± 0.27 and 0.19 ± 0.07 W m^{-2}, respectively. The forcing from OC is close to another study[36] from the same location, which reported −1.1 ± 0.4 W m^{-2} for BrC at TOA. Figure 4 shows the frequency distribution of CF along with wavelength integrated forcing due to BC + absorbing shell and only lensing effect. Forcing due to lensing is defined as the difference in forcing due to BC + absorbing shell and that due to only BC. The forcing from BC + shell mainly depends upon the coating factor and to a lesser extent on the net refractive index of the shell. The average CF of 1.5 induces a net forcing of 0.097 ± 0.04 W m^{-2} for a BC + absorbing shell assumption, which is less than pure BC forcing (0.19 W m^{-2}) because of the increased scattering as a result of the thick shell. However, for a small coating (CF = 1.2), forcing due to BC + shell is 0.33 ± 0.06 W m^{-2}, in which the contribution from the lensing effect alone is 0.13 ± 0.06 W m^{-2}, indicating warming that is close to a global modeling study[6] value of 0.1 W m^{-2} based on AERONET network data. As the CF increases above 1.35, the

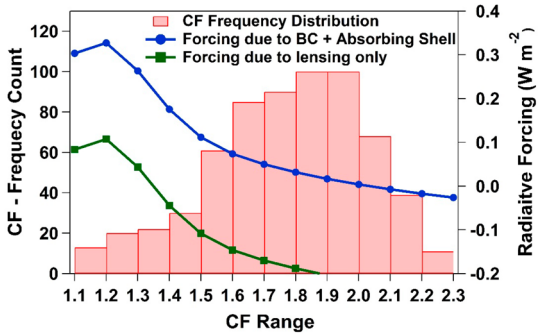

Figure 4. Frequency distribution of CF along with the wavelength-integrated radiative forcing due to BC + absorbing shell and lensing effect only.

scattering dominates over absorption, thereby creating a cooling effect as a result of the lensing effect. A study by Saleh et al.[18] on a global scale reports a 0.29 W m^{-2} warming from the lensing effect as a result of absorbing OC at 550 nm, which is higher than the values reported in this study mainly as a result of higher shell thickness, which scatters light.

Because a spherical shape and perfect core−shell structure are assumed in this study, the Mie theory is used to derive aerosol optical properties to calculate forcing. Primarily emitted particles might not be spherical in shape. However, in this study, aerosols were measured at the Indian Institute of Technology (IIT) Kanpur campus, where open burning is prohibited and the majority of sampled aerosols are from outside and/or undergo long-range transportation. We assume aerosols collected during this study to be aged by at least 5 to 6 h. This aging time scale increases the possibility for the formation of spherical particles and coating assumption made in this study.[46] A major fraction of organics in the sampling location is highly oxygenated, contributing less to absorption when compared to primary organics. Still, the radiative forcing values show an overall smaller cooling as a result of BrC and thinly coated aerosols. Therefore, for regions dominated with primary organic aerosols, BrC can induce TOA warming. The findings of this study reiterate the importance of considering BrC absorption and the lensing effect in global climate models.

■ ASSOCIATED CONTENT

Supporting Information

The Supporting Information is available free of charge on the ACS Publications website at DOI: 10.1021/acsearthspacechem.7b00074.

Details of the materials and methods, including instrumentation, PMF analysis, van Krevelen diagram, and uncertainty analysis (PDF)

■ AUTHOR INFORMATION

Corresponding Author

*Telephone: +91-512 2597845. E-mail: snt@iitk.ac.in.

ORCID

N. Rastogi: 0000-0003-4532-7827

S. N. Tripathi: 0000-0002-6402-4680

Notes

The authors declare no competing financial interest.

DOI: 10.1021/acsearthspacechem.7b00074
ACS Earth Space Chem. 2018, 2, 31−37

■ ACKNOWLEDGMENTS

The authors acknowledge Tarun Gupta of IIT Kanpur, India for the PM_1 sampler. The authors thank Anil Mandaria and Vipul Lalchandani of IIT Kanpur for collecting and analyzing PM_1 filters in Kanpur. The authors also acknowledge IIT Kanpur for providing them with HR-ToF-AMS for PG research and teaching. The authors gratefully acknowledge the financial support given by the Earth System Science Organization, Ministry of Earth Sciences, Government of India (Grant MM/NERCMoES-03/2014/002), to conduct this research under Monsoon Mission.

■ REFERENCES

(1) Bond; Doherty, S. J.; Fahey, D. W.; Forster, P. M.; Berntsen, T.; DeAngelo, B. J.; Flanner, M. G.; Ghan, S.; Kärcher, B.; Koch, D.; Kinne, S.; Kondo, Y.; Quinn, P. K.; Sarofim, M. C.; Schultz, M. G.; Schulz, M.; Venkataraman, C.; Zhang, H.; Zhang, S.; Bellouin, N.; Guttikunda, S. K.; Hopke, P. K.; Jacobson, M. Z.; Kaiser, J. W.; Klimont, Z.; Lohmann, U.; Schwarz, J. P.; Shindell, D.; Storelvmo, T.; Warren, S. G.; Zender, C. S. Bounding the role of black carbon in the climate system: A scientific assessment. *J. Geophys. Res.: Atmos.* **2013**, *118* (11), 5380−5552.

(2) Andreae, M. O.; Gelencsér, A. Black carbon or brown carbon? The nature of light-absorbing carbonaceous aerosols. *Atmos. Chem. Phys.* **2006**, *6* (10), 3131−3148.

(3) Bond, T. C.; Streets, D. G.; Yarber, K. F.; Nelson, S. M.; Woo, J. H.; Klimont, Z. A technology-based global inventory of black and organic carbon emissions from combustion. *J. Geophys. Res.: Atmos.* **2004**, *109*, D14203.

(4) Chung, C. E.; Ramanathan, V.; Decremer, D. Observationally constrained estimates of carbonaceous aerosol radiative forcing. *Proc. Natl. Acad. Sci. U. S. A.* **2012**, *109* (29), 11624−11629.

(5) Myhre, G.; Shindell, D.; Bréon, F.-M.; Collins, W.; Fuglestvedt, J.; Huang, J.; Koch, D.; Lamarque, J.-F.; Lee, D.; Mendoza, B.; Nakajima, T.; Robock, A.; Stephens, G.; Takemura, T.; Zhang, H. In *Climate Change 2013: The Physical Science Basis. Contribution of Working Group I to the Fifth Assessment Report of the Intergovernmental Panel on Climate Change*; Stocker, T. F., Qin, D., Plattner, G.-K., Tignor, M., Allen, S. K., Boschung, J., Nauels, A., Xia, Y., Bex, V., Midgley, P. M., Eds.; Cambridge University Press: New York, 2013; pp 659−740.

(6) Feng, Y.; Ramanathan, V.; Kotamarthi, V. R. Brown carbon: A significant atmospheric absorber of solar radiation? *Atmos. Chem. Phys.* **2013**, *13* (17), 8607−8621.

(7) Bond, T. C.; Bergstrom, R. W. Light absorption by carbonaceous particles: An investigative review. *Aerosol Sci. Technol.* **2006**, *40* (1), 27−67.

(8) Bond, T. C.; Habib, G.; Bergstrom, R. W. Limitations in the enhancement of visible light absorption due to mixing state. *J. Geophys. Res.: Atmos.* **2006**, *111*, D20211.

(9) Fuller, K. A. Scattering and absorption cross sections of compounded spheres. III. Spheres containing arbitrarily located spherical inhomogeneities. *J. Opt. Soc. Am. A* **1995**, *12* (1995), 893−904.

(10) Jo, D. S.; Park, R. J.; Lee, S.; Kim, S. W.; Zhang, X. A global simulation of brown carbon: Implications for photochemistry and direct radiative effect. *Atmos. Chem. Phys.* **2016**, *16* (5), 3413−3432.

(11) Wang, X.; Heald, C. L.; Ridley, D. A.; Schwarz, J. P.; Spackman, J. R.; Perring, A. E.; Coe, H.; Liu, D.; Clarke, A. D. Exploiting simultaneous observational constraints on mass and absorption to estimate the global direct radiative forcing of black carbon and brown carbon. *Atmos. Chem. Phys.* **2014**, *14* (20), 10989−11010.

(12) Park, R. J.; Kim, M. J.; Jeong, J. I.; Youn, D.; Kim, S. A contribution of brown carbon aerosol to the aerosol light absorption and its radiative forcing in East Asia. *Atmos. Environ.* **2010**, *44* (11), 1414−1421.

(13) Lin, G.; Penner, J. E.; Flanner, M. G.; Sillman, S.; Xu, L.; Zhou, C. Radiative forcing of organic aerosol in the atmosphere and on snow: Effects of SOA and brown carbon. *J. Geophys. Res.: Atmos.* **2014**, *119* (12), 7453−7476.

(14) Liu, J.; Scheuer, E.; Dibb, J.; Ziemba, L. D.; Thornhill, K. L.; Anderson, B. E.; Wisthaler, A.; Mikoviny, T.; Devi, J. J.; Bergin, M.; Weber, R. J. Brown carbon in the continental troposphere. *Geophys. Res. Lett.* **2014**, *41* (6), 2191−2195.

(15) Kirillova, E. N.; Andersson, A.; Tiwari, S.; Srivastava, A. K.; Bisht, D. S.; Gustafsson, Ö. Water-soluble organic carbon aerosols during a full New Delhi winter: Isotope-based source apportionment and optical properties. *J. Geophys. Res.: Atmos.* **2014**, *119* (6), 3476−3485.

(16) Srinivas, B.; Sarin, M. M. Brown carbon in atmospheric outflow from the Indo-Gangetic Plain: Mass absorption efficiency and temporal variability. *Atmos. Environ.* **2014**, *89*, 835−843.

(17) Srinivas, B.; Rastogi, N.; Sarin, M. M.; Singh, A.; Singh, D. Mass absorption efficiency of light absorbing organic aerosols from source region of paddy-residue burning emissions in the Indo-Gangetic Plain. *Atmos. Environ.* **2016**, *125* (Part B), 360−370.

(18) Saleh, R.; Marks, M.; Heo, J.; Adams, P. J.; Donahue, N. M.; Robinson, A. L. Contribution of brown carbon and lensing to the direct radiative effect of carbonaceous aerosols from biomass and biofuel burning emissions. *J. Geophys. Res.: Atmos.* **2015**, *120* (19), 10,285−10,296.

(19) Kirchstetter, T. W.; Novakov, T.; Hobbs, P. V. Evidence that the spectral dependence of light absorption by aerosols is affected by organic carbon. *J. Geophys. Res.: Atmos.* **2004**, *109*, D21208.

(20) Lack, D. A.; Langridge, J. M.; Bahreini, R.; Cappa, C. D.; Middlebrook, A. M.; Schwarz, J. P. Brown carbon and internal mixing in biomass burning particles. *Proc. Natl. Acad. Sci. U. S. A.* **2012**, *109*, 14802−14807.

(21) Liu, J.; Bergin, M.; Guo, H.; King, L.; Kotra, N.; Edgerton, E.; Weber, R. J. Size-resolved measurements of brown carbon in water and methanol extracts and estimates of their contribution to ambient fine-particle light absorption. *Atmos. Chem. Phys.* **2013**, *13* (24), 12389−12404.

(22) Alexander, D. T. L.; Crozier, P. A.; Anderson, J. R. Brown Carbon Spheres in East Asian Outflow and Their Optical Properties. *Science* **2008**, *321* (5890), 833−836.

(23) Saleh, R.; Robinson, E. S.; Tkacik, D. S.; Ahern, A. T.; Liu, S.; Aiken, A. C.; Sullivan, R. C.; Presto, A. A.; Dubey, M. K.; Yokelson, R. J.; Donahue, N. M.; Robinson, A. L. Brownness of organics in aerosols from biomass burning linked to their black carbon content. *Nat. Geosci.* **2014**, *7* (9), 647−650.

(24) Zhang, X.; Kim, H.; Parworth, C. L.; Young, D. E.; Zhang, Q.; Metcalf, A. R.; Cappa, C. D. Optical Properties of Wintertime Aerosols from Residential Wood Burning in Fresno, CA: Results from DISCOVER-AQ 2013. *Environ. Sci. Technol.* **2016**, *50* (4), 1681−1690.

(25) Shamjad, P. M.; Tripathi, S. N.; Aggarwal, S. G.; Mishra, S. K.; Joshi, M.; Khan, A.; Sapra, B. K.; Ram, K. Comparison of Experimental and Modeled Absorption Enhancement by Black Carbon (BC) Cored Polydisperse Aerosols under Hygroscopic Conditions. *Environ. Sci. Technol.* **2012**, *46* (15), 8082−8089.

(26) World Health Organization (WHO). *WHO Air Quality Guidelines for Particulate Matter, Ozone, Nitrogen Dioxide and Sulfur Dioxide*; WHO: Geneva, Switzerland, 2005.

(27) Middlebrook, A. M.; Bahreini, R.; Jimenez, J. L.; Canagaratna, M. R. Evaluation of Composition-Dependent Collection Efficiencies for the Aerodyne Aerosol Mass Spectrometer using Field Data. *Aerosol Sci. Technol.* **2012**, *46* (3), 258−271.

(28) Sullivan, A. P.; Weber, R. J.; Clements, A. L.; Turner, J. R.; Bae, M. S.; Schauer, J. J. A method for on-line measurement of water-soluble organic carbon in ambient aerosol particles: Results from an urban site. *Geophys. Res. Lett.* **2004**, *31* (13), L13105.

(29) Satish, R.; Shamjad, P.; Thamban, N.; Tripathi, S.; Rastogi, N. Temporal Characteristics of Brown Carbon over the Central Indo-Gangetic Plain. *Environ. Sci. Technol.* **2017**, *51* (12), 6765−6772.

(30) Nakayama, T.; Sato, K.; Matsumi, Y.; Imamura, T.; Yamazaki, A.; Uchiyama, A. Wavelength and NOx dependent complex refractive

DOI: 10.1021/acsearthspacechem.7b00074
ACS Earth Space Chem. 2018, 2, 31−37

index of SOAs generated from the photooxidation of toluene. *Atmos. Chem. Phys.* **2013**, *13* (2), 531−545.
(31) Sun, H. L.; Biedermann, L.; Bond, T. C. Color of brown carbon: A model for ultraviolet and visible light absorption by organic carbon aerosol. *Geophys. Res. Lett.* **2007**, *34* (17), L17813.
(32) Birch, M. E.; Cary, R. A. Elemental Carbon-Based Method for Monitoring Occupational Exposures to Particulate Diesel Exhaust. *Aerosol Sci. Technol.* **1996**, *25* (3), 221−241.
(33) Thamban, N. M.; Tripathi, S. N.; Moosakutty, S. P.; Kuntamukkala, P.; Kanawade, V. P. Internally mixed black carbon in the Indo-Gangetic Plain and its effect on absorption enhancement. *Atmos. Res.* **2017**, *197*, 211−223.
(34) Mätzler, C. *MATLAB Functions for Mie Scattering and Absorption*; Institut für Angewandte Physik: Bern, Switzerland, 2002; Research Report 2002-08.
(35) Dinar, E.; Abo Riziq, A.; Spindler, C.; Erlick, C.; Kiss, G.; Rudich, Y. The complex refractive index of atmospheric and model humic-like substances (HULIS) retrieved by a cavity ring down aerosol spectrometer (CRD-AS). *Faraday Discuss.* **2008**, *137*, 279−295.
(36) Shamjad, P. M.; Tripathi, S. N.; Pathak, R.; Hallquist, M.; Arola, A.; Bergin, M. H. Contribution of Brown Carbon to Direct Radiative Forcing over the Indo-Gangetic Plain. *Environ. Sci. Technol.* **2015**, *49* (17), 10474−10481.
(37) Dey, S.; Tripathi, S. N. Estimation of aerosol optical properties and radiative effects in the Ganga basin, northern India, during the wintertime. *J. Geophys. Res.* **2007**, *112*, D03203.
(38) Chen, Y.; Bond, T. C. Light absorption by organic carbon from wood combustion. *Atmos. Chem. Phys.* **2010**, *10* (4), 1773−1787.
(39) Paatero, P.; Tapper, U. Positive matrix factorization: A non-negative factor model with optimal utilization of error estimates of data values. *Environmetrics* **1994**, *5* (2), 111−126.
(40) Jimenez, J. L.; Canagaratna, M. R.; Donahue, N. M.; Prevot, A. S. H.; Zhang, Q.; Kroll, J. H.; DeCarlo, P. F.; Allan, J. D.; Coe, H.; Ng, N. L.; Aiken, A. C.; Docherty, K. S.; Ulbrich, I. M.; Grieshop, A. P.; Robinson, A. L.; Duplissy, J.; Smith, J. D.; Wilson, K. R.; Lanz, V. A.; Hueglin, C.; Sun, Y. L.; Tian, J.; Laaksonen, A.; Raatikainen, T.; Rautiainen, J.; Vaattovaara, P.; Ehn, M.; Kulmala, M.; Tomlinson, J. M.; Collins, D. R.; Cubison, M. J.; Dunlea, J.; Huffman, J. A.; Onasch, T. B.; Alfarra, M. R.; Williams, P. I.; Bower, K.; Kondo, Y.; Schneider, J.; Drewnick, F.; Borrmann, S.; Weimer, S.; Demerjian, K.; Salcedo, D.; Cottrell, L.; Griffin, R.; Takami, A.; Miyoshi, T.; Hatakeyama, S.; Shimono, A.; Sun, J. Y.; Zhang, Y. M.; Dzepina, K.; Kimmel, J. R.; Sueper, D.; Jayne, J. T.; Herndon, S. C.; Trimborn, A. M.; Williams, L. R.; Wood, E. C.; Middlebrook, A. M.; Kolb, C. E.; Baltensperger, U.; Worsnop, D. R. Evolution of Organic Aerosols in the Atmosphere. *Science* **2009**, *326* (5959), 1525−1529.
(41) Shamjad, P. M.; Tripathi, S. N.; Thamban, N. M.; Vreeland, H. Refractive Index and Absorption Attribution of Highly Absorbing Brown Carbon Aerosols from an Urban Indian City-Kanpur. *Sci. Rep.* **2016**, *6*, 37735.
(42) Heald, C. L.; Kroll, J. H.; Jimenez, J. L.; Docherty, K. S.; DeCarlo, P. F.; Aiken, A. C.; Chen, Q.; Martin, S. T.; Farmer, D. K.; Artaxo, P. A simplified description of the evolution of organic aerosol composition in the atmosphere. *Geophys. Res. Lett.* **2010**, *37* (8), L08803.
(43) Lee, H. J.; Aiona, P. K.; Laskin, A.; Laskin, J.; Nizkorodov, S. A. Effect of Solar Radiation on the Optical Properties and Molecular Composition of Laboratory Proxies of Atmospheric Brown Carbon. *Environ. Sci. Technol.* **2014**, *48* (17), 10217−10226.
(44) Laskin, A.; Laskin, J.; Nizkorodov, S. A. Chemistry of Atmospheric Brown Carbon. *Chem. Rev.* **2015**, *115* (10), 4335−4382.
(45) Chakrabarty, R. K.; Moosmüller, H.; Chen, L. W. A.; Lewis, K.; Arnott, W. P.; Mazzoleni, C.; Dubey, M. K.; Wold, C. E.; Hao, W. M.; Kreidenweis, S. M. Brown carbon in tar balls from smoldering biomass combustion. *Atmos. Chem. Phys.* **2010**, *10* (13), 6363−6370.
(46) Gustafsson, Ö.; Ramanathan, V. Convergence on climate warming by black carbon aerosols. *Proc. Natl. Acad. Sci. U. S. A.* **2016**, *113* (16), 4243−4245.

DOI: 10.1021/acsearthspacechem.7b00074
ACS Earth Space Chem. 2018, 2, 31−37